

RD-R142 840

EFFECT OF RADIAL LOAD DISTRIBUTION ON THE  
FIRST-HARMONIC INFLOW VELOCITY O. (U) DAVID W TAYLOR  
NAVAL SHIP RESEARCH AND DEVELOPMENT CENTER BET.

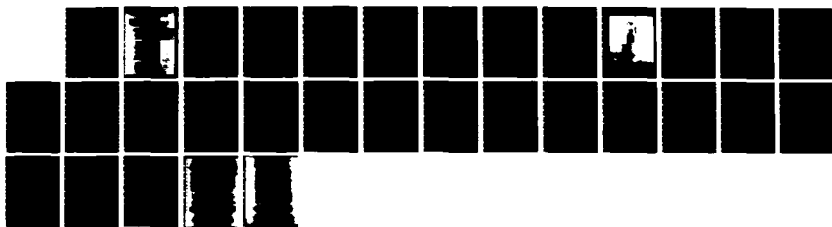
1/1

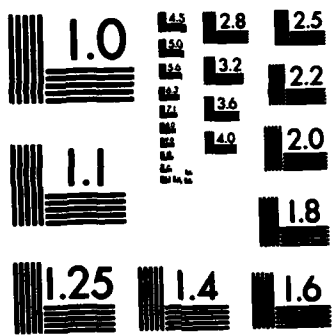
UNCLASSIFIED

H R CHAPLIN APR 84 DTNSRDC/ASED-84/03

F/G 12/1

NL





MICROCOPY RESOLUTION TEST CHART  
NATIONAL BUREAU OF STANDARDS-1963-A

AD-A142 840



EFFECT OF RADIAL LOAD DISTRIBUTION ON THE FIRST HARMONIC  
INFLOW VELOCITY OF A HELICOPTER ROTOR  
AT TRANSITION SPEEDS

by

Harvey R. Chaplin

APPROVED FOR PUBLIC RELEASE:  
DISTRIBUTION UNLIMITED

LAND SURFACE EFFECTS DEPARTMENT

DTNSRDC/ASED-84/03

APRIL 1984

DAVID  
W.  
TAYLOR  
NAVAL  
SHIP  
RESEARCH  
AND  
DEVELOPMENT  
CENTER

BETHESDA  
MARYLAND  
20084

ETIC  
ELECTRONIC  
TECHNOLOGY  
INSTITUTE

JULY 11 1984

84 OR 10 0

**UNCLASSIFIED**

SECURITY CLASSIFICATION OF THIS PAGE (When Data Entered)

<b>REPORT DOCUMENTATION PAGE</b>		<b>READ INSTRUCTIONS BEFORE COMPLETING FORM</b>
1. REPORT NUMBER <b>DTNSRDC/ASED-84/03</b>	2. GOVT ACCESSION NO. <b>AD-A242 870</b>	3. RECIPIENT'S CATALOG NUMBER
4. TITLE (and Subtitle) <b>EFFECT OF RADIAL LOAD DISTRIBUTION ON THE FIRST-HARMONIC INFLOW VELOCITY OF A HELICOPTER ROTOR AT TRANSITION SPEEDS</b>	5. TYPE OF REPORT & PERIOD COVERED	
7. AUTHOR(s)  <b>Harvey R. Chaplin</b>	6. PERFORMING ORG. REPORT NUMBER	
9. PERFORMING ORGANIZATION NAME AND ADDRESS <b>David Taylor Naval Ship R&amp;D Center Aviation and Surface Effects Department Bethesda, Maryland 20084</b>	10. PROGRAM ELEMENT, PROJECT, TASK AREA & WORK UNIT NUMBERS <b>Program Element 62766N Task Area ZF66412001 1-1660-825</b>	
11. CONTROLLING OFFICE NAME AND ADDRESS <b>David Taylor Naval Ship R&amp;D Center Office of Technical Director Bethesda, Maryland 20084</b>	12. REPORT DATE <b>April 1984</b>	
14. MONITORING AGENCY NAME & ADDRESS (if different from Controlling Office)	13. NUMBER OF PAGES <b>28</b>	
16. DISTRIBUTION STATEMENT (of this Report)  <b>APPROVED FOR PUBLIC RELEASE: DISTRIBUTION UNLIMITED</b>	15. SECURITY CLASS. (of this report) <b>UNCLASSIFIED</b>	
17. DISTRIBUTION STATEMENT (of the abstract entered in Block 20, if different from Report)		
18. SUPPLEMENTARY NOTES		
19. KEY WORDS (Continue on reverse side if necessary and identify by block number) <b>Circulation Control Rotor Helicopter Transition Performance Rotor Load Distributions</b>		
20. ABSTRACT (Continue on reverse side if necessary and identify by block number)  <b>A joint Navy/NASA experimental investigation was conducted in October 1983 in the Langley Research Center VSTOL Wind Tunnel to test the hypothesis that helicopters with unusually hub-weighted radial load distributions should experience a more severe first harmonic inflow velocity field during transition than ordinary helicopters. This report presents an approximate analysis of the experimental results. The hypothesis is strongly supported. Compared to the rotor configuration with the most tip-weighted load</b> <b>(Continued on reverse side)</b>		

**UNCLASSIFIED**

SECURITY CLASSIFICATION OF THIS PAGE (When Data Entered)

(Block 20 continued)

distribution, the configuration with the most hub-weighted distribution appears to have experienced an approximately 50 percent greater first-harmonic inflow at a 50 percent greater critical flight speed.

**UNCLASSIFIED**

SECURITY CLASSIFICATION OF THIS PAGE(When Data Entered)

## TABLE OF CONTENTS

	Page
<b>LIST OF FIGURES . . . . .</b>	<b>iii</b>
<b>TABLE . . . . .</b>	<b>iii</b>
<b>NOTATION . . . . .</b>	<b>iv</b>
<b>ABSTRACT . . . . .</b>	<b>1</b>
<b>ADMINISTRATIVE INFORMATION . . . . .</b>	<b>1</b>
<b>INFORMATION . . . . .</b>	<b>1</b>
<b>EXPERIMENTS . . . . .</b>	<b>2</b>
<b>AERODYNAMICS PERFORMANCE CODE . . . . .</b>	<b>4</b>
<b>ANALYTICAL PROCEDURE . . . . .</b>	<b>7</b>
<b>RESULTS AND DISCUSSION . . . . .</b>	<b>12</b>
<b>ACKNOWLEDGMENTS . . . . .</b>	<b>14</b>
<b>REFERENCES . . . . .</b>	<b>23</b>

## LIST OF FIGURES

<b>1 - Rotor Model in Langley Research Center 4- by 7-Meter Wind Tunnel . . . . .</b>	<b>3</b>
<b>2 - Comparison of Measured and Calculated Thrust . . . . .</b>	<b>6</b>
<b>3 - Comparison of Measured and Calculated Hub Moments . . . . .</b>	<b>8</b>
<b>4 - Effect of Variation in Input Values of <math>K_{lam}</math> and <math>\psi_f</math> on Calculated First-Harmonic Components of Root Flapping Moment . . . . .</b>	<b>11</b>
<b>5 - Normalized First-Harmonic Inflow versus Normalized Advance Ratio . . . . .</b>	<b>15</b>
<b>6 - Calculated Blade Load Distribution on Advancing and Retreating Blades at a Near-Critical Speed . . . . .</b>	<b>17</b>
<b>7 - Normalized First-Harmonic Inflow versus Normalized Advance Ratio Compared with Heuristically Modified Theory . . . . .</b>	<b>20</b>
 <hr/>	
<b>Table 1 - Experimental and Calculated Results . . . . .</b>	<b>21</b>

## NOTATION

$B_0$	Mean blade root duct pressure, psig
$B_1$	Amplitude of first-harmonic blade root duct pressure, psi
$C_T$	Thrust coefficient, $T/(\pi \rho R^2 V_{tip}^2)$
$K_{\lambda_{am}}$	Nondimensional correlation parameter, $\lambda_1^*/\lambda_1^\dagger$
$M_f$	Amplitude of first-harmonic blade root flapping moment, ft-lb
$M_{fc}$	$M_f \cos (\psi_f)$
$R$	Rotor radius, ft
$r$	Radial coordinate from hub center, ft
$T$	Thrust, lb
$V_k$	Free-stream velocity, knots
$V_o$	Free-stream velocity, ft/sec
$V_{tip}$	Tip speed, ft/sec
$w$	Inflow velocity normal to disk, ft/sec
$\alpha_s$	Shaft angle, deg
$\theta$	Collective blade angle, deg
$\lambda$	Inflow ratio, $w/V_{tip}$
$\lambda_o$	Mean value of $\lambda$
$\lambda_1$	First-harmonic cosine component of $\lambda$
$\mu$	Advance ratio, $V_o/V_{tip}$
$\mu^*$	Normalized value of $\mu$ , $\mu/\sqrt{C_T}/2$
$\lambda_o^*$	Normalized value of $\lambda_o$ , $\lambda_o/\sqrt{C_T}/2$
$\lambda_1^*$	Normalized value of $\lambda_1$ , $\lambda_1/\sqrt{C_T}/2$

$\lambda_0^*$  Value of  $\lambda_0^*$  predicted by Reference 1  
 $\lambda_1^*$  Value of  $\lambda_1^*$  predicted by Reference 1  
 $\rho$  Ambient air density, slugs/ft<sup>3</sup>  
 $\psi_f$  Azimuthal phase angle of  $M_f$ , deg  
 $\psi_p$  Azimuthal phase angle of  $B_l$ , deg

Accession For	
NTIS GRA&I	<input checked="" type="checkbox"/>
DTIC TAB	<input type="checkbox"/>
Unannounced	<input type="checkbox"/>
Justification	
Distribution	
Availability Codes	
All and/or	
Not for Special	

A1

## ABSTRACT

A joint Navy/NASA experimental investigation was conducted in October 1983 in the Langley Research Center VSTOL Wind Tunnel to test the hypothesis that helicopters with unusually hub-weighted radial load distributions should experience a more severe first-harmonic inflow velocity field during transition than ordinary helicopters. This report presents an approximate analysis of the experimental results. The hypothesis is strongly supported. Compared to the rotor configuration with the most tip-weighted load distribution, the configuration with the most hub-weighted distribution appears to have experienced an approximately 50 percent greater first-harmonic inflow at a 50 percent greater critical flight speed.

## ADMINISTRATIVE INFORMATION

This analysis and the Navy participation in the experiments on which it is based were funded by the Independent Exploratory Development Program. The experiments were performed in the 4- by 7-Meter Wind Tunnel at the Langley Research Center courtesy of the National Aeronautics and Space Administration (NASA).

## INTRODUCTION

In late 1979, flight tests were undertaken by Kaman Aerospace Corporation on an H-2 helicopter equipped with an experimental circulation control rotor (XH-2/CCR). It was found to be much more difficult to trim the helicopter in pitch at low speeds than anticipated; in fact, the flight tests were eventually abandoned with no flights at speeds exceeding the critical transition speed.

Although a number of problems were found which could qualitatively explain the pitch trim difficulty, it was hypothesized that, because the radial load distribution on a circulation control rotor is much more hub-centered than that on an ordinary rotor, the transition inflow field at critical speed might be more severe. Although analyses of the flights completed did not indicate unusual inflow characteristics, the possibility remained that unusual effects, including a higher-than-normal critical transition speed, might have shown up had further flights at higher speeds been possible.

In 1983, an agreement was reached between the David Taylor Naval Ship Research and Development Center (DTNSRDC) and the National Aeronautics and Space Administration to conduct experiments in the Langley Research Center (LRC) VSTOL Wind Tunnel to seek evidence concerning possible effects of radial load distribution on the transition inflow field. These experiments were completed in October 1983 by a joint LRC/DTNSRDC team using an existing DTNSRDC circulation control rotor model. This report presents an approximate analysis of the results.

#### EXPERIMENTS

The rotor model was 80-in. in diameter with four, 5-in.-chord blades. These blades were judged small enough to yield reasonably valid transition data in the LRC VSTOL Wind Tunnel (Figure 1). The model was equipped with a pneumatic valve system capable of providing blade duct mean pressures up to 10 psig and azimuthal 1-per-rev harmonic variation of the pressure of amplitude up to about 60 percent of the mean. The valve characteristic was such that a 2-per-rev harmonic variation one-third the amplitude of the 1-per-rev component and 90 deg out of phase with it also resulted. The model was equipped with blade duct pressure transducers, blade root flapping moment strain gages, and azimuth reference signal generators. A more complete description of the model is given in Reference 1.

The model was mounted on a four-component DTNSRDC load cell balance designed to measure thrust, pitching moment, rolling moment, and yawing moment during hover tests. All tests were performed at a tip speed of 500 ft/sec. The thrust reading of this balance was also to be used for the forward flight tests. Unfortunately, the balance system malfunctioned during early hover tests. Enough data, however, were acquired before the malfunction to confirm that the model was functioning properly and to establish an approximate correlation between the first-harmonic flapping moment strain gage measurements and the actual root (hub-center) flapping moment. All analyses of the transition data then had to be performed in terms of root flapping moment.

A tabulation of the experimental results for the transition inflow analyses is presented in Table 1. In addition to the tabulated data, a number of other data channels were recorded including the azimuth angle of the maximum opening

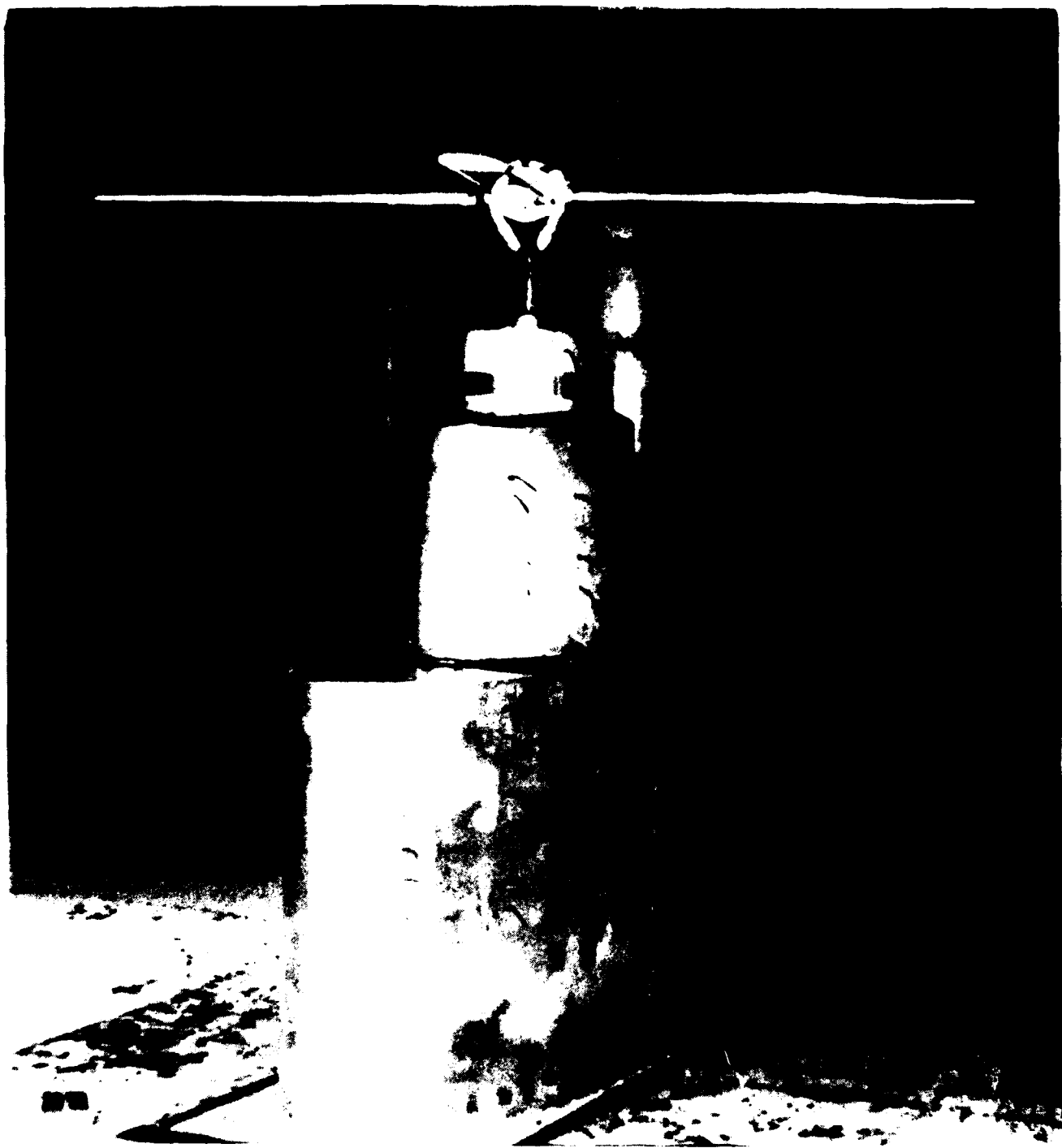


Figure 1 - Rotor Model in Langley Research Center  
4- by 7-Meter Wind Tunnel

of the pneumatic valve (which was of the eccentric-circular-cam type) and the output of blade duct pressure transducers located at the tip and a mid-radius position, in addition to the "blade root" (10 percent-radius) transducer output used in the analysis. Comparison of the first-harmonic phase angles of these various quantities with each other and with the recorded cam angle reveals random inconsistencies in the phase angles on the order of  $\pm 10$  deg. Since LRC was unable to provide on-site reduction of the high-speed data, the unusually large error band was not detected in time to initiate efforts to identify and correct the cause.

In addition to the random inconsistencies, there are also regular inconsistencies—notably that the recorded phase angle (i.e., azimuthal position of first-harmonic peak) of the duct pressure at the blade tip lags that at the root by about 3 deg on average; whereas, due to the time lag involved in near-sonic transport of a pressure signal from root to tip, the blade root first-harmonic pressure peak should lead that at the tip by about 23 deg. The results of the analyses suggest that the recorded tip pressure phase is more nearly correct.

#### AERODYNAMICS PERFORMANCE CODE

The performance code used in the analyses is an undocumented code developed by the author on an HP-9836 desk computer for quick-look investigations of the effects of various design parameters on the performance of circulation control and X-Wing rotors. The code employs a curve-fit approximation to the experimentally determined two-dimensional characteristics of the circulation control airfoils used on this model rotor, including Reynolds number and compressibility effects. It also employs a "distributed momentum" variation of the approximate inflow equations presented by Blake and White.<sup>2</sup> The Blake and White formulation can be written as:

$$\lambda = [\lambda_0^{\pm} + \lambda_1^{\pm} r/R \cos (\psi)] \sqrt{C_T/2} \quad (1)$$

where

$$\lambda_0^{\pm} = \sqrt{(\sqrt{4+\mu^4} - \mu^2)/2} \quad (2)$$

$$\lambda_1^{\pm} = \sqrt{8\mu^*/(\sqrt{4+\mu^4} + \mu^2)} \quad (3)$$

The "distributed momentum" variation merely replaces the quantity  $\lambda_0^{\pm}$  by the quantity  $\lambda_0^{\pm}\sqrt{(\text{local disk loading})/(\text{average disk loading})}$ .

In the present investigation, a further modification was introduced. The quantity  $\lambda_1^{\pm}$  was replaced by the quantity  $K_{\text{lam}}\lambda_1^{\pm}$  so that the first-harmonic inflow term could be easily varied iteratively (by varying  $K_{\text{lam}}$ ) to determine what value of this term was needed for best correlation with the experimental results. For purposes of this investigation, the "rigid rotor" option of the code was used; that is, elastic deflections of the blade were neglected.

It was intended to validate the aerodynamics performance code (and, if needed, make empirical adjustments to it) by comparing calculated to measured thrust and hub moments in hover at three blade angles and several combinations of blade duct mean and cyclic pressure. As previously mentioned, only one collective angle was completed before the thrust balance malfunctioned, and only a few cyclic pressures at that collective angle were completed before the hub moment balance began to behave erratically.

Correlation of the few valid thrust data points with previous measurements (unpublished) and with the calculated behavior is shown in Figure 2. It is concluded that (1) the model was functioning properly, and (2) the thrust predictions from the aerodynamics performance code are satisfactory.

The few valid hub moment measurements were used to establish the approximate relationship:

$$\text{Mean Hub Moment} \doteq 2.5 M_{fe}$$

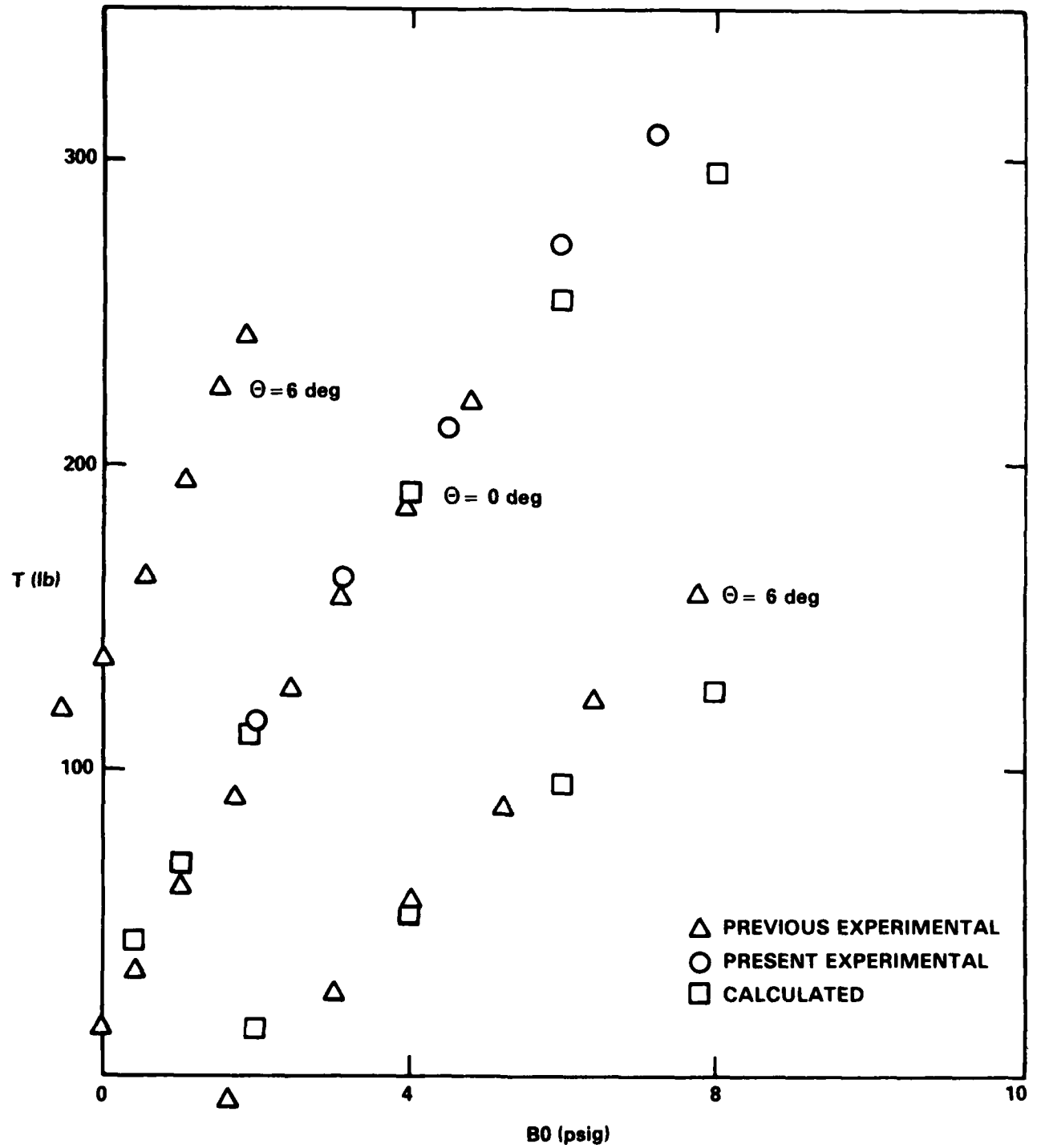


Figure 2 - Comparison of Measured and Calculated Thrust  
 $(V_k = 0, V_{tip} = 500 \text{ fps})$

where  $M_{fe}$  is the first-harmonic amplitude of measured flapping moment (measured by a strain gage bridge at the 12-percent radius station). From this it is deduced that:

$$M_f \doteq 1.25 M_{fe}$$

where  $M_f$  is the root (hub center) flapping moment. This relationship was employed in all subsequent analyses.

Correlation of the measured flapping moments with calculated behavior is shown in Figure 3. The flapping moment predictions from the aerodynamics performance code are also satisfactory. Consequently, empirical adjustments to the code were not needed.

#### ANALYTICAL PROCEDURE

No inflow quantities were directly measured in the experiment. The plan was to determine for each experimental data point the value of

$$\lambda_1^* = K_{\text{lam}} \lambda_1^{\ddagger}$$

which, when substituted for  $\lambda_1^{\ddagger}$  in Equation (1), would yield agreement between the measured and calculated first-harmonic root flapping moment amplitude and phase ( $M_f, \psi_f$ ). The calculation would have employed the measured values of root pressure zeroth, first- and second-harmonic amplitude and first- and second-harmonic phase.

In view of the random and systematic irregularities in the pressure phase measurements, this plan was modified slightly:

1. It was assumed that the best first estimate of actual effective root pressure phase was a value leading the measured phase by 20 deg.
2. From this estimate, random variations on the order of  $\pm 10$  deg can be expected.
3. To reduce the time required for analysis, it was decided to define "agreement" by:

Figure 3 - Comparison of Measured and Calculated Hub Moments

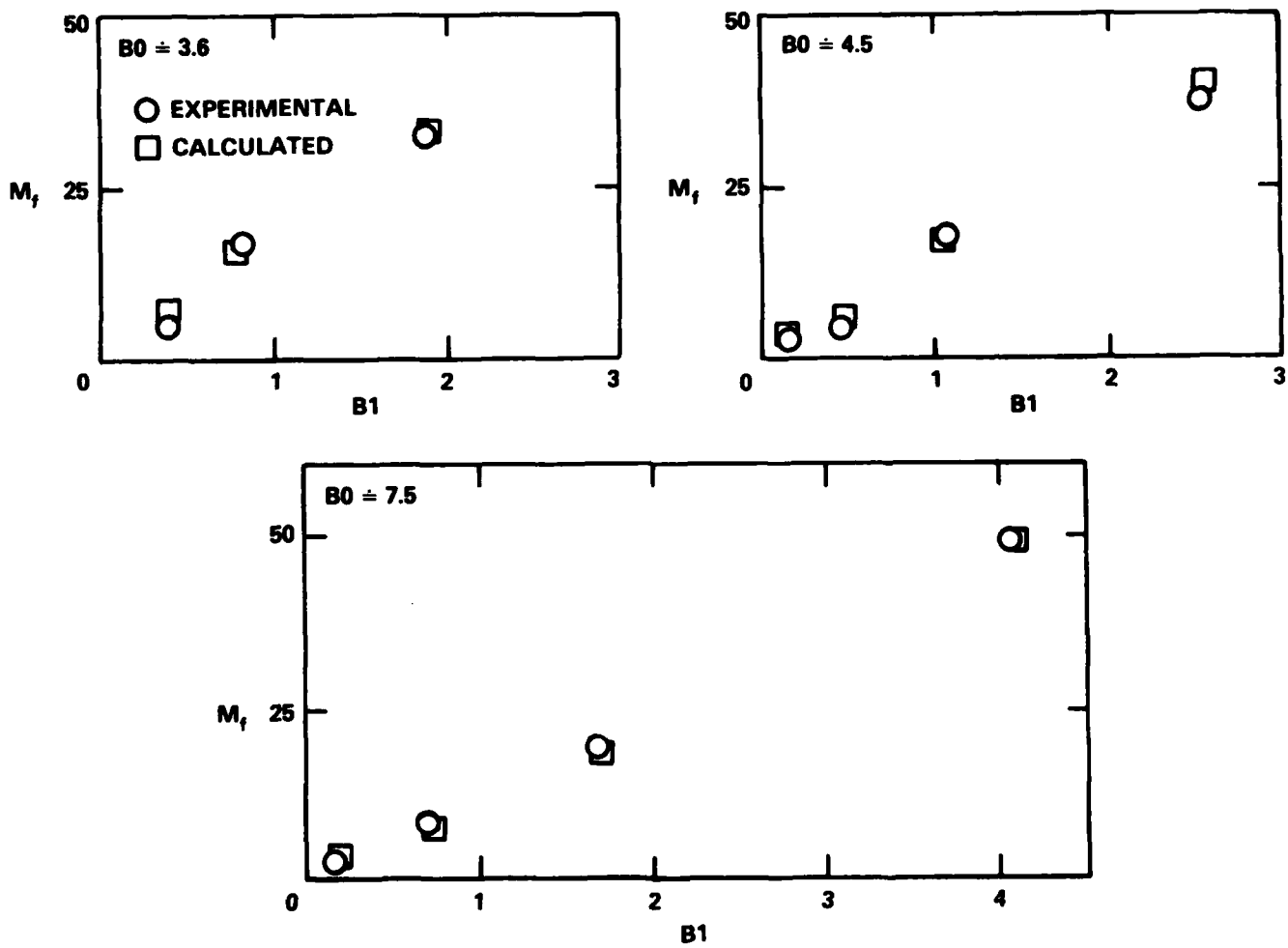


Figure 3a -  $\theta = -3$  Degrees

Figure 3 (Continued)

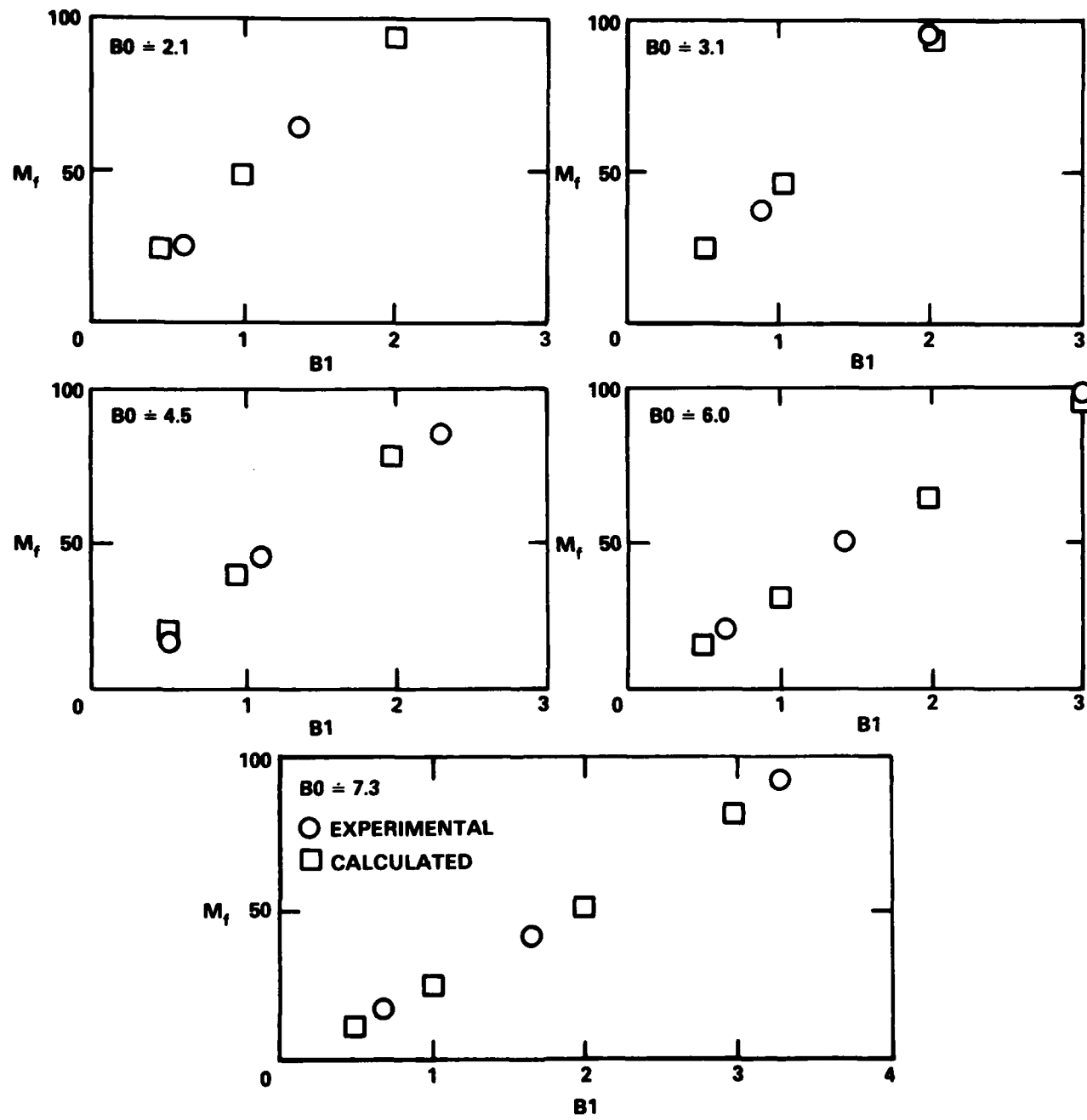


Figure 3b -  $\theta = 0$  Degrees

- a. Measured  $M_f \cos \psi_f$  = Calculated  $M_f \cos \psi_f$ .
- b. Discrepancies between measured  $\psi_p$  and calculated input  $\psi_p$  should both be "reasonable" in light of the above-discussed data irregularities.

These regrettably soft criteria may become more understandable in light of the example presented in Figure 4. Here the experimental results for Run 61/Test Point 1 are shown with the calculated results for various combinations of input pressure phase,  $\psi_p$ , and input inflow correlation parameter,  $K_{\lambda\text{am}}$ . Note that the "reasonable" range of input  $\psi_p$  (+1 deg - 20  $\pm$  10 deg = -9 to -29 deg) brackets the input  $\psi_p$  of -12 deg required to produce agreement in both  $M_f \cos \psi_f$  and  $M_f \sin \psi_f$ . More importantly, note that the value of  $K_{\lambda\text{am}}$  required to produce agreement in  $M_f \cos \psi_f$  alone is rather insensitive to small errors in either  $\psi_f$  or  $\psi_p$ . This insensitivity to errors in  $\psi_p$  prevails so long as  $\psi_p$  is near zero (or 180 deg), and the insensitivity to errors in  $\psi_f$  prevails so long as  $\psi_f$  is near 180 deg (or zero). Fortunately, a goodly fraction of the data were taken under conditions meeting both of these criteria, tending to strengthen what would otherwise be very low confidence in the results of the analyses.

In view of the data uncertainties and the rather time-consuming calculation procedure (about 10 min per calculated point), the actual analysis procedure did not use an orderly grid of calculated points such as illustrated in Figure 4. Rather, from a first guess at  $\psi_p$  and  $K_{\lambda\text{am}}$ , subsequent iterative estimates (usually two or three) were made until the result was judged "close enough," and the last estimate was recorded in Table 1. Thus, these estimates could be improved upon by further analysis, if desired.

The second-harmonic pressure amplitudes and phases are not recorded in Table 1; in all cases, they are close to one-third the amplitude of the first-harmonic and 90 deg out of phase. The second-harmonic component is included in the calculations. The effect of the second-harmonic component is to make the pressure wave broad/flat on top and narrow/peaky on the bottom.

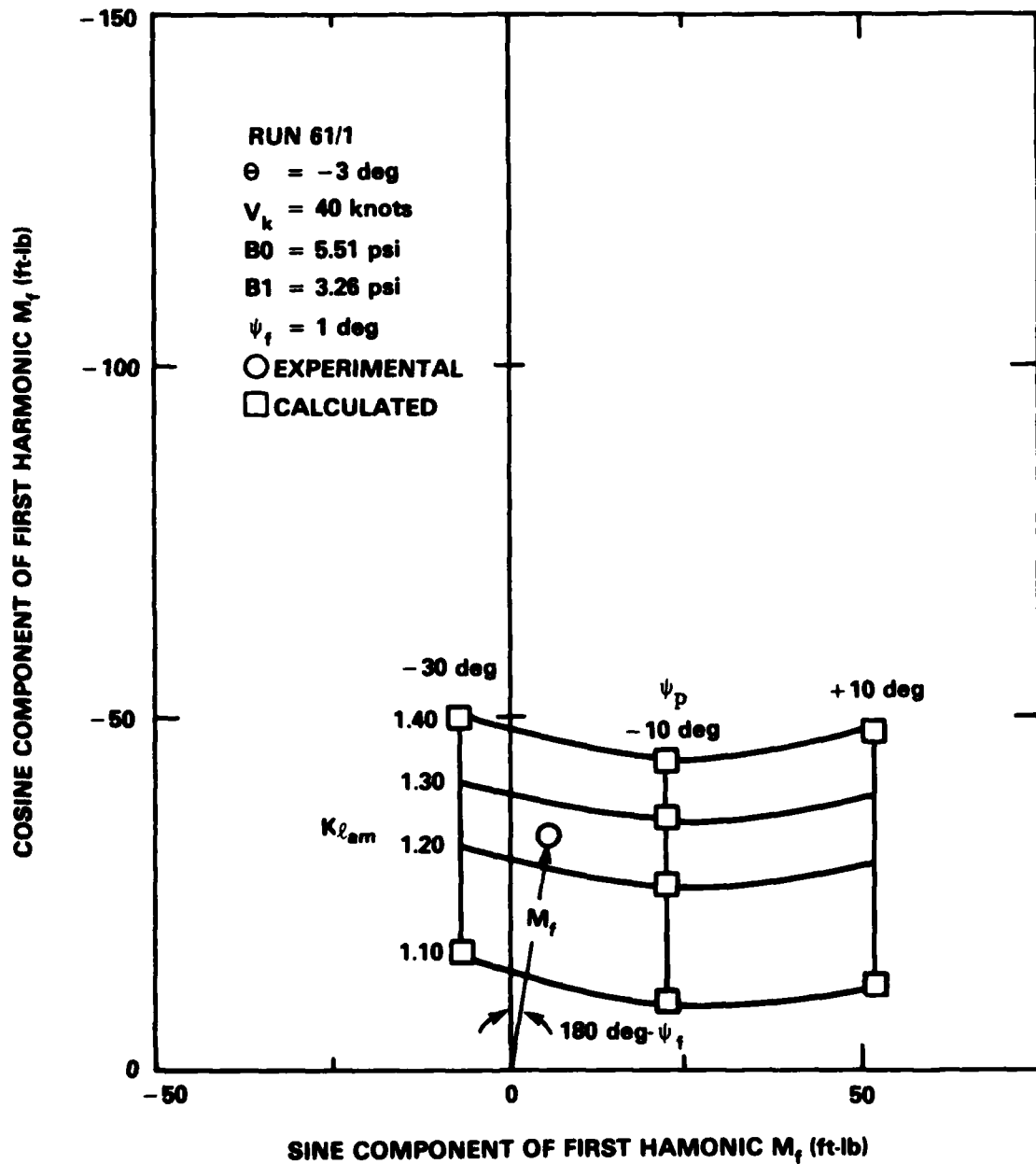


Figure 4 - Effect of Variation in Input Values of  $K_{lam}$  and  $\psi_f$  on Calculated First-Harmonic Components of Roof Flapping Moment

## RESULTS AND DISCUSSION

The results are summarized as plots of  $\lambda_1^*$  versus  $\mu^*$  in Figure 5. There is a systematic variation with collective blade angle, with the results for  $\theta = 0$  deg falling in reasonably good agreement with the predictions of Reference 1. The results for  $\theta = -3$  deg and  $\theta = -6$  deg, however, fall progressively further above the predictions of Reference 1. This is consistent with the original hypothesis that the first-harmonic inflow term might be greater for rotors with relatively hub-weighted radial load distributions.

Figure 6 shows the calculated blade load per foot at the advancing ( $\psi = 90$  deg) and retreating ( $\psi = 270$  deg) blade positions for two thrust coefficients at each of the blade collective angles. At  $\theta = 0$  deg, blade loading tends to increase with increasing radius over most of the blade (as it does for all conventional rotors); at  $\theta = -3$  deg, the blade loading is approximately constant over most of the blade; and at  $\theta = -6$  deg, blade loading decreases rapidly with increasing radius over the outer half radius.

The theory of Reference 1 is a rather heuristic one. It represents the wing-like component of rotor lift, as determined from simple momentum theory, by a horseshoe vortex of span equal to rotor diameter and estimates  $\lambda_1$  from the normal-to-disk induced velocities of this vortex system on the centerline at the disk leading and trailing edges. If these simple assumptions give a correct estimate for an ordinary rotor (i.e., one with heavily tip-weighted radial load distribution), it might be assumed that a similar estimate using a horseshoe vortex of span less than rotor diameter would be more appropriate for a rotor with a heavily hub-weighted radial load distribution. Alternatively, this speculation can be expressed in the form that such a rotor should behave (for purposes of first-order inflow estimates) like an ordinary rotor at the same thrust but reduced diameter; or like an ordinary rotor of the same diameter but greater thrust coefficient. Such an estimate is achieved by plotting  $K\lambda_1^*$  versus  $K\mu^*$ ,  $K > 1$ , where  $\lambda_1^*$  ( $\mu^*$ ) is taken from Equations (1) through (3).

Such estimates are compared to the results of Figure 5 in Figure 7. Values of  $K = 1.25$  and  $K = 1.53$  are found to correlate the  $\theta = -3$  deg and  $\theta = -6$  deg data, respectively. (The constants 1.25 and 1.53 were selected purely to fit the data and not from any theoretical considerations.) The degree of data fit

achieved in this way does tend to support these heuristic arguments and suggests that some further simple theoretical explorations seeking to connect the constant K to the radial load distribution in a quantitative way might be productive.

Because of the substantial uncertainties surrounding the experimental data, it is necessary to question whether any reasonable systematic error could produce the trend exhibited in Figure 7 artificially. The most obvious such possibility, since there was no valid measurement of thrust during the transition tests, is the possibility of a systematic error in the calculated thrust. If the calculation procedure systematically underestimated the thrust at  $\theta = -6$  deg and/or overestimated the thrust at  $\theta = 0$  deg, an artificial difference similar to that displayed in Figure 7 would result. However, to produce the magnitude of difference shown in Figure 7 would require that

$$\left( \frac{\text{Calculated thrust } @ \theta = 0 \text{ deg}}{\text{Actual thrust } @ \theta = 0 \text{ deg}} \right) : \left( \frac{\text{Calculated thrust } @ \theta = -6 \text{ deg}}{\text{Actual thrust } @ \theta = -6 \text{ deg}} \right)$$

be equal to  $1.53^2 = 2.33$ . This is regarded as extremely unlikely.

A second possibility is that the decision to base the analysis on root (hub-center) flapping moment which, in turn, was estimated as  $1.25 \times$  (measured flapping moment at 12-percent radius) might produce a systematic error. However, re-analysis of a typical data point at each  $\theta$  was performed in terms of the measured 12-percent radius flapping moment (with no additional calibration factor applied). The result was to reduce the estimated value of  $\lambda_1^*$  by about 3 percent in each case. In other words, there was no effect on the trend displayed in Figure 7.

It is concluded that, although significant quantitative errors are possible, the trend displayed in Figure 7 is almost surely real, and rotors with unusually hub-centered radial load distributions do indeed experience unusually severe transition inflow fields.

#### ACKNOWLEDGMENTS

The author wishes to thank Mr. Gary R. Smith and Mr. Kenneth A. Phillips of DTNSRDC for planning and monitoring the experiments and for reducing the experimental data. Thanks also are extended to those personnel from the NASA Langley Research Center and the Army Structures Laboratory who assisted in the testing program. The contributions of Mr. John D. Berry and Mr. Arthur E. Phelps of the Army Structures Laboratory were especially helpful in carrying out the experiments in the LRC 4- by 7-Meter Wind Tunnel.

Figure 5 - Normalized First-Harmonic Inflow  
versus Normalized Advance Ratio

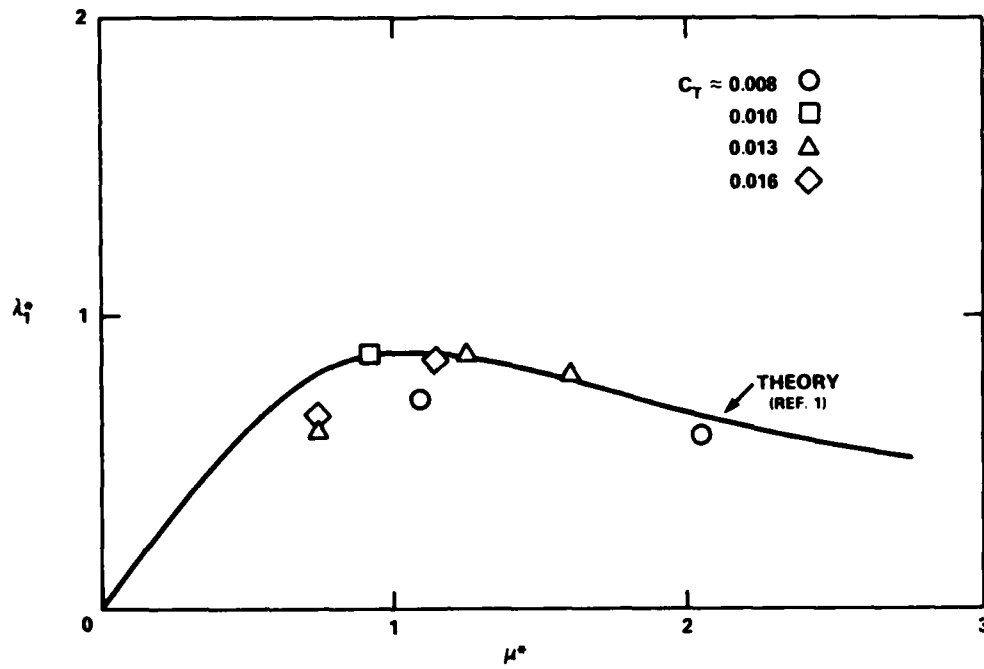


Figure 5a -  $\theta = 0$  Degrees

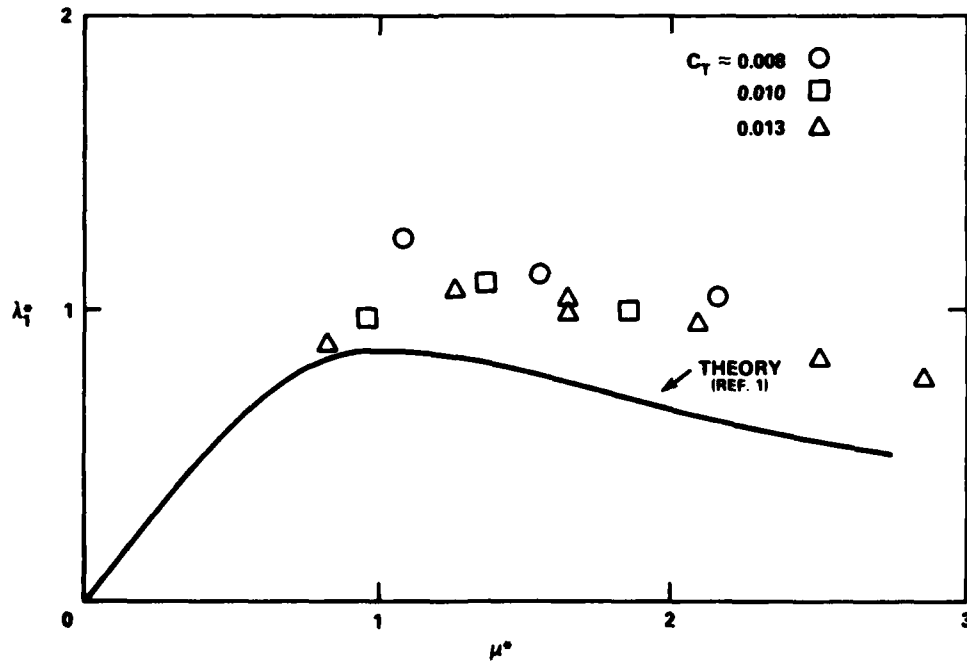


Figure 5b -  $\theta = -3$  Degrees

Figure 5 (Continued)

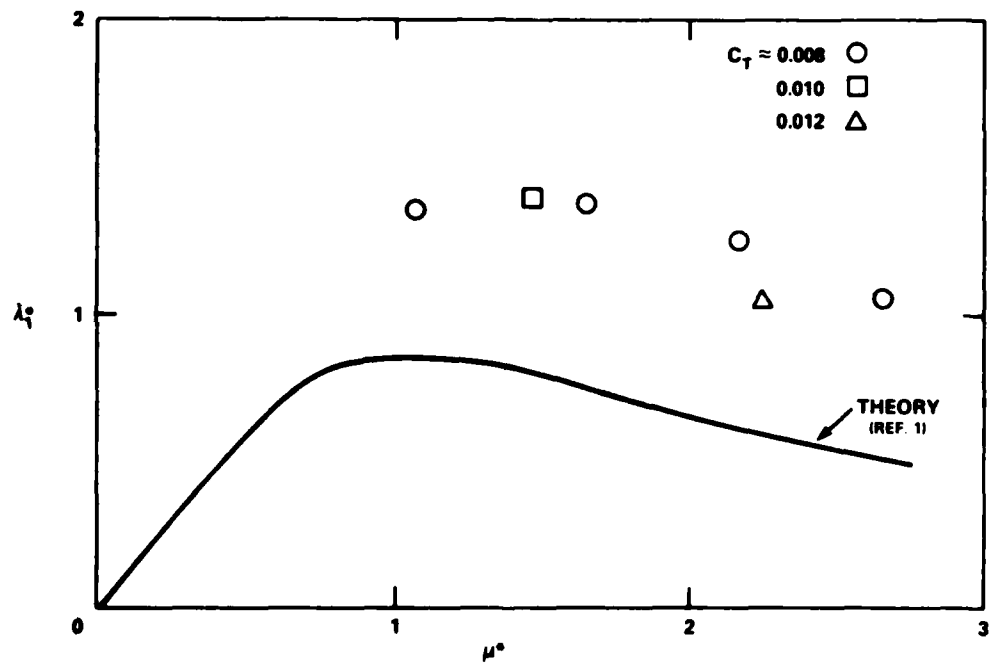


Figure 5c -  $\theta = -6$  Degrees

Figure 6 - Calculated Blade Load Distribution on Advancing and Retreating Blades at a Near-Critical Speed

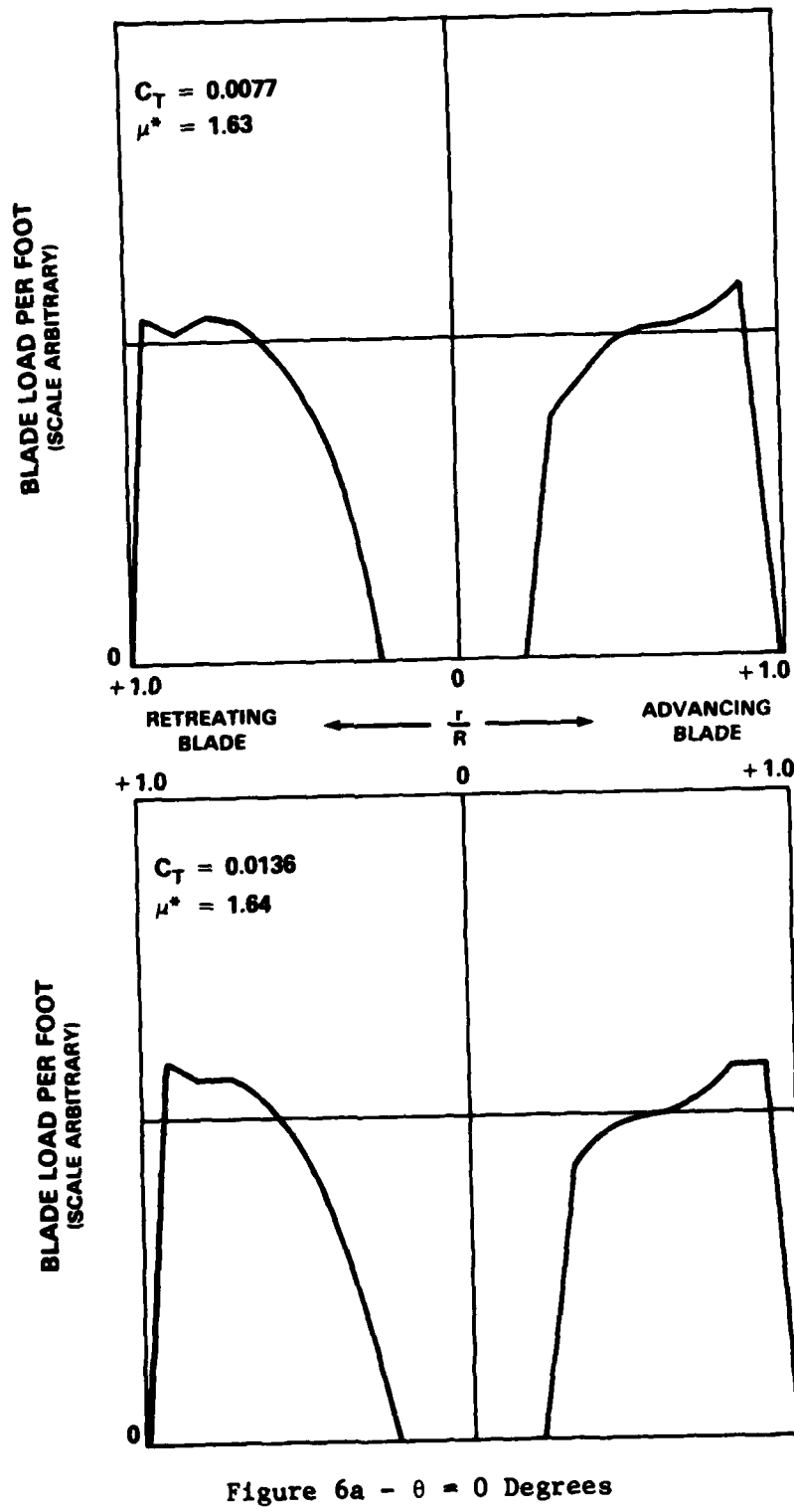


Figure 6a -  $\theta = 0$  Degrees

Figure 6 (Continued)

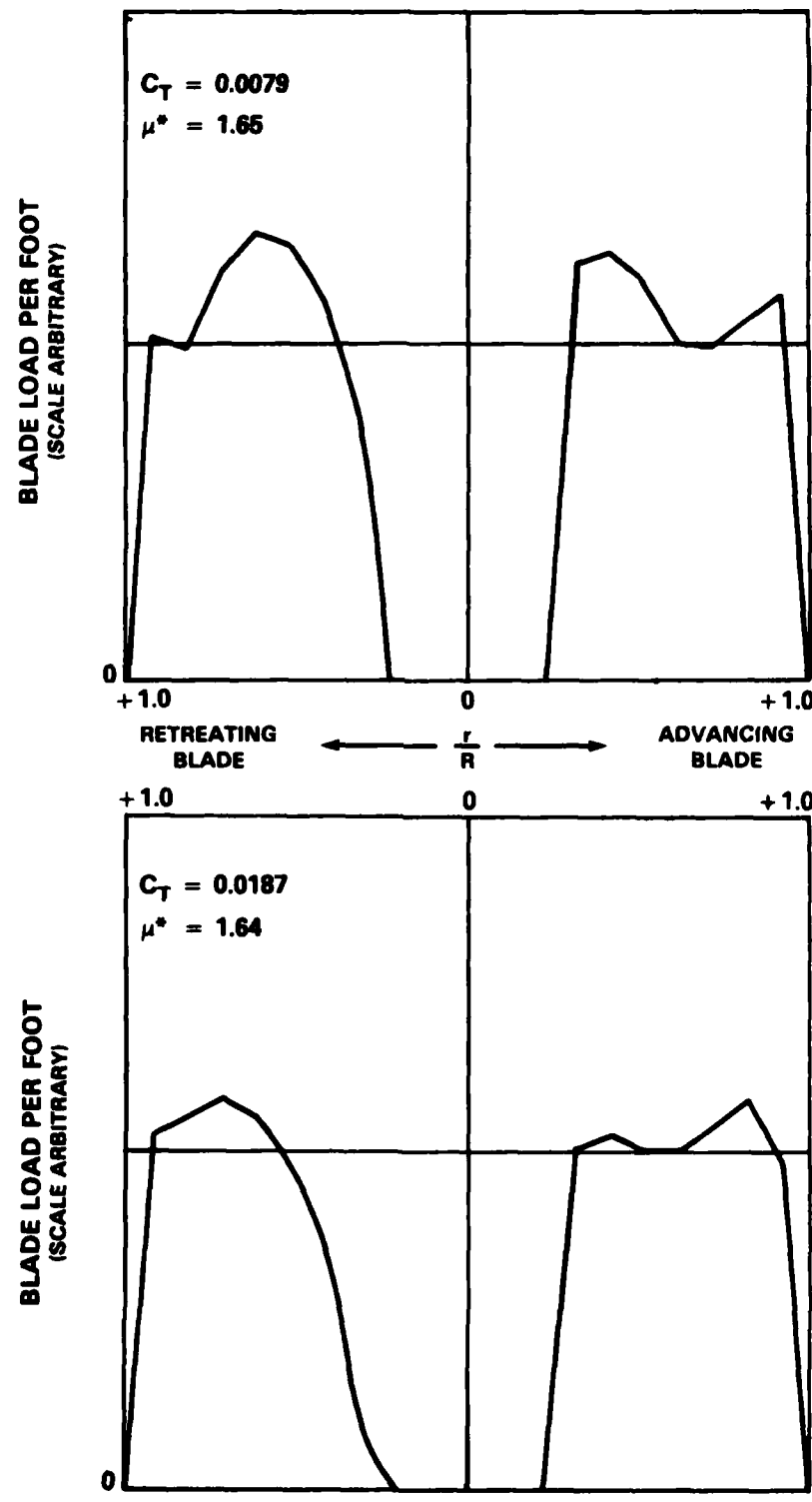


Figure 6b -  $\theta = -3$  Degrees

Figure 6 (Continued)

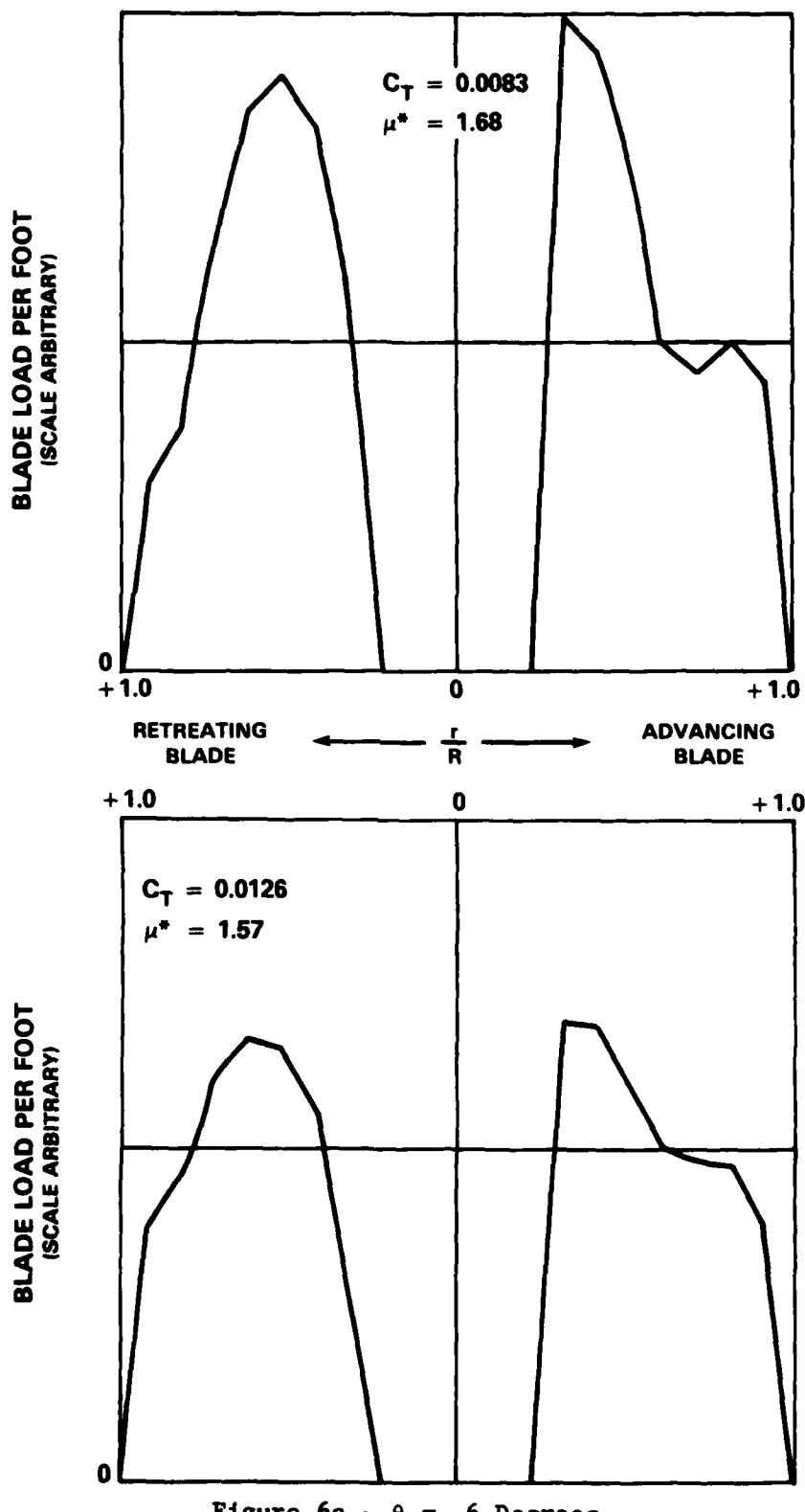


Figure 6c -  $\theta = -6$  Degrees

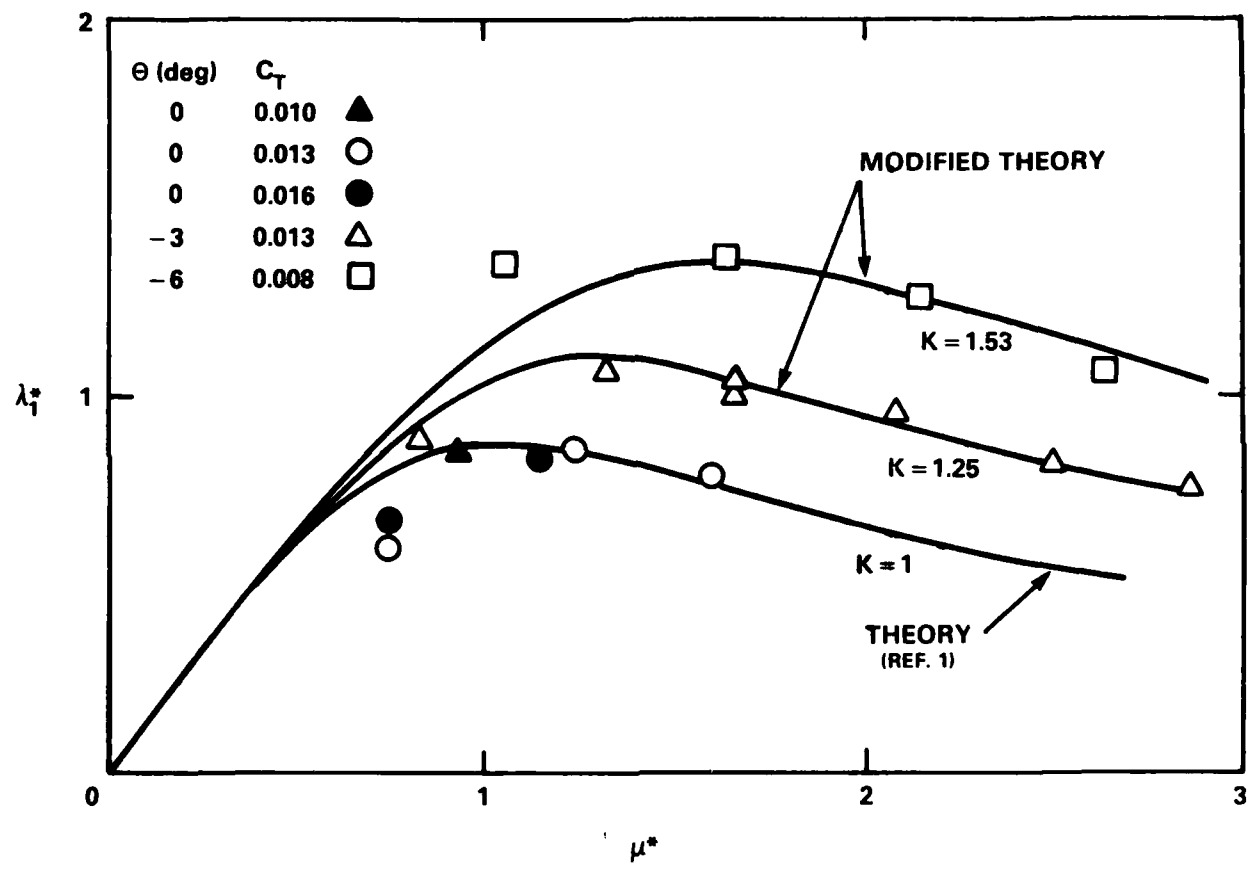


Figure 7 - Normalized First-Harmonic Inflow versus Normalized Advance Ratio  
Compared with Heuristically Modified Theory

TABLE 1 - EXPERIMENTAL AND CALCULATED RESULTS  
 $(V_{tip} = 500 \text{ ft/sec}, \alpha_s = 0 \text{ deg})$

RUN/TP	$\theta$	Experimental						Calculated							
		$V_k$	$B\theta$	B1	$\psi_p$	$M_f$	$\psi_f$	$M_{fc}$	$\psi_p$	$M_f$	$\psi_f$	$M_{fc}$	$10^4 C_T$	$\mu^*$	$\lambda_1^*$
51/4	0	19.9	1.57	1.04	9	19	154	-17	-5	18	146	-15	76	1.09	0.70
51/5	19.1	2.84	1.80	25	29	126	-17	5	29	128	-18	100	0.91	0.86	
51/6	18.3	4.04	2.44	4	13	103	-3	-5	16	103	-4	119	0.80	0.73	
51/7	18.3	5.91	3.39	-5	4	327	3	-15	9	63	4	143	0.73	0.60	
51/8	20.0	7.82	4.32	4	9	149	-8	-20	11	134	-8	160	0.74	0.64	
51/11	30.2	3.67	2.27	10	30	148	-25	-10	34	138	-26	138	1.23	0.86	
51/12	29.7	5.07	3.02	11	29	149	-25	-15	32	139	-24	158	1.13	0.83	
51/13	39.0	0.86	0.66	-6	26	182	-26	-15	30	153	-25	84	2.04	0.58	
51/14	39.5	2.99	1.93	6	29	160	-28	-20	32	149	-28	139	1.60	0.79	
53/5	-3	20.5	5.38	3.29	17	14	185	-14	-18	13	199	-13	98	0.97	0.96
53/4	19.8	3.63	2.32	23	24	161	-23	-5	24	164	-23	77	1.08	1.23	
53/7	20.0	9.76	5.37	17	31	198	-30	-23	30	182	-30	136	0.82	0.88	
54/3	30.0	3.25	2.15	18	28	186	-28	-20	28	195	-27	86	1.55	1.11	
54/5	30.0	6.55	3.98	24	41	201	-38	-25	39	188	-39	130	1.26	1.07	
54/4	30.0	4.78	2.90	10	32	194	-31	-20	31	185	-31	110	1.37	1.09	
55/2	40.0	5.62	3.55	6	40	195	-39	-25	38	184	-38	134	1.65	1.03	
61/3	40.1	2.41	1.67	5	28	160	-27	-10	27	173	-27	79	2.16	1.04	
61/1	40.0	5.51	3.26	1	34	169	-33	-9	42	145	-34	133	1.65	0.99	
61/2	40.5	3.74	2.38	-1	27	155	-25	-10	29	154	-26	108	1.85	0.99	
60/5	50.0	4.27	2.53	-13	29	168	-28	-18	33	148	-28	134	2.08	0.95	
59/1	60.0	4.74	2.86	-5	23	152	-20	-15	26	142	-20	132	2.50	0.82	
58/4	70.0	4.25	2.54	-13	23	130	-15	-23	21	144	-16	133	2.87	0.77	

TABLE 1 (Continued)

Experimental							Calculated								
RUN/TP	$\theta$	$V_k$	$B\phi$	B1	$\psi_p$	$M_f$	$\psi_f$	$M_{fc}$	$\psi_p$	$M_f$	$\psi_f$	$M_{fc}$	$10^4 C_T$	$\mu^*$	$\lambda_1^*$
68/4	-6	19.8	7.68	4.42	16	33	21.1	-28	-10	20	179	-27	83	1.04	1.35
69/3	30.0	5.42	3.33	-1	36	21.6	-29	-15	32	196	-30	78	1.62	1.39	
69/4	30.1	7.47	4.40	20	52	20.3	-48	-15	45	183	-45	99	1.44	1.40	
70/3	40.0	4.93	3.11	1	34	224	-25	-15	27	203	-25	79	2.15	1.27	
71/4	49.8	7.00	3.72	-10	44	203	-41	-20	41	184	-41	115	2.22	1.05	
71/3	49.8	4.80	2.95	9	29	243	-13	-15	16	214	-13	82	2.63	1.05	

#### REFERENCES

1. Reader, K.R., "Hover Evaluation of a Circulation Control High Speed Rotor," David Taylor Naval Ship R&D Center Report 77-0034 (Jun 1977).
2. Blake, B.B. and F. White, "Improved Method of Predicting Helicopter Control Response and Gust Sensitivity," American Helicopter Society Preprint No. 79-25 (May 1979).

DTNSRDC ISSUES THREE TYPES OF REPORTS

1. DTNSRDC REPORTS, A FORMAL SERIES, CONTAIN INFORMATION OF PERMANENT TECHNICAL VALUE. THEY CARRY A CONSECUTIVE NUMERICAL IDENTIFICATION REGARDLESS OF THEIR CLASSIFICATION OR THE ORIGINATING DEPARTMENT.
2. DEPARTMENTAL REPORTS, A SEMIFORMAL SERIES, CONTAIN INFORMATION OF A PRIMARY, TEMPORARY, OR PROPRIETARY NATURE OR OF LIMITED INTEREST OR SIGNIFICANCE. THEY CARRY A DEPARTMENTAL ALPHANUMERICAL IDENTIFICATION.
3. TECHNICAL MEMORANDA, AN INFORMAL SERIES, CONTAIN TECHNICAL DOCUMENTATION OF LIMITED USE AND INTEREST. THEY ARE PRIMARILY WORKING PAPERS INTENDED FOR INTERNAL USE. THEY CARRY AN IDENTIFYING NUMBER WHICH INDICATES THEIR TYPE AND ALPHANUMERICAL CODE OF THE ORIGINATING DEPARTMENT. ANY DISTRIBUTION OUTSIDE DTNSRDC MUST BE APPROVED BY THE HEAD OF THE ORIGINATING DEPARTMENT ON A CASE-BY-CASE BASIS.

SEARCHED

FILMED

8

261

SEARCHED